Molecular Crystals and Liquid Crystals

ISSN: 1542-1406 (Print) 1563-5287 (Online) Journal homepage: http://www.tandfonline.com/loi/gmcl20

Molecular Design of Carbazole-based Dyes and the Influence of Alkyl Substituent on the Performance of Dye-Sensitized Solar Cells

A. S. Beni, M. Zarandi, A. R. Madram, Y. Bayat, A. N. Chermahini & R. Ghahary

To cite this article: A. S. Beni, M. Zarandi, A. R. Madram, Y. Bayat, A. N. Chermahini & R. Ghahary (2016) Molecular Design of Carbazole-based Dyes and the Influence of Alkyl Substituent on the Performance of Dye-Sensitized Solar Cells, Molecular Crystals and Liquid Crystals, 629:1, 29-43, DOI: 10.1080/15421406.2015.1106895

To link to this article: http://dx.doi.org/10.1080/15421406.2015.1106895

Published online: 16 Jun 2016.

MOLECULAR CRYSTALS AND LIQUID CRYSTALS
2016, VOL. 629, 29–43
http://dx.doi.org/10.1080/15421406.2015.1106895

Taylor & Francis
Taylor & Francis Group

Molecular design of carbazole-based dyes and the influence of alkyl substituent on the performance of dye-sensitized solar cells

A. S. Beni[a], M. Zarandi[a], A. R. Madram[b], Y. Bayat[b], A. N. Chermahini[c], and R. Ghahary[d]

[a]Department of Chemistry, Faculty of Science, Yasouj University, Yasouj, Iran; [b]Department of Chemistry and Chemical Engineering, Malek Ashtar University, Tehran, Iran; [c]Department of Chemistry, Isfahan University of Technology, Isfahan, Iran; [d]Department of Physics, Sharif University, Tehran, Iran

ABSTRACT

Carbazole is an alternant polycyclic aromatic hydrocarbon consisting of three fused rings with a large, aromatic system, containing nitrogen atom showing extensive electron delocalization. In this work, carbazole applied as π-conjugated bridge to construct electron donor–π–electron acceptor (D–π–A) organic dyes, where barbutiric acid and thiazolidine-2,4-dione as electron acceptor. The effects of these three acceptors and length of alkyl on the performance of the DSSCs were investigated systematically along with their photophysical and photo electrochemical properties. These series of organic dyes include (B-CH, B-C B, DT-CB, DB-CB). Our investigation indicate among dyes containing butyl as same donor, DT-CB exhibited the maximum overall conversion efficiency of 1.44% and from dyes by deferent electron donor B-CH shows conversion efficiency of 1.47%.

KEYWORDS

Dye-sensitized solar cells (DSSCs); barbutiric acid; alkyl; carbazole

1. Introduction

Today's one of the most urgent in energy field is finding good resource replacement for traditional and commonly used source of energy. Therefore to accomplish this purpose application of solar energy is highly desirable because it has so many advantages. The Sun is an obvious source of clean and cheap energy. Photovoltaic technologies harness the power of sun. Among known Photovoltaic technologies, dye-sensitized solar cells (DSSCs), developed by Grätzel and co-workers, have attracted so many attention in two past decades due to their promising potential to actualize solar-to-electricity conversion. This generation of solar cells overcomes the problems such as requirement of high costs and highly energy consuming preparation methods of old generation. Two basic actions in the dye-sensitized solar cell (DSSC) include: the charge generation is done at the semiconductor-dye interface and the semiconductor and the electrolyte do the charge transport. Therefore, one crucial component of solar cells is photosensitizer. Great academic efforts have been fuscous on synthesis of versatile dyes [1–12]. Metal complexes based on ruthenium and zinc have been extensively studied for DSSCs and high efficiencies over 10%–11% [13,14] and 12% [15] have been obtained. Nevertheless, these metals have some problems such as high cost, relatively low molar extinction coefficients and

CONTACT A. S. Beni salimibeni@mail.yu.ac.ir
Color versions of one or more of the figures in the article can be found online at www.tandfonline.com/gmcl.

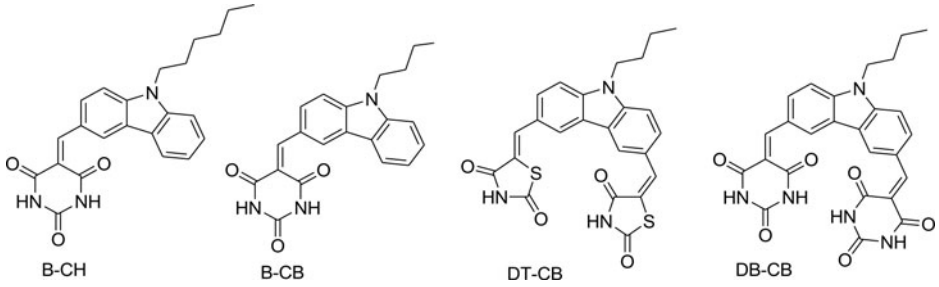

Scheme 1. Chemical structure of novel dye B-CH, B-C B, DT-CB, and DB-CB

rarity. Organic dyes show higher molar extinction coefficients, and need only simple synthesis and purification processes at lower cost, therefore tremendous investigation have been done to their development in all over the world. Some of these photosensitizers include different group such as coumarin [16–18], merocyanine [19], indoline [20,21], polyene [22], hemicyanine [23,24], fluorene [25–26], triphenylamine (TPA) [27–36], tetrahydroqui-noline [37,38], carbazole [39,40], and heteroanthracene (phenothiazine (PTZ) and phenoxazine (POZ)) [41–47] and so on. Generally, organic dyes in order to act as photosensitizer should contain an electron donor—π bridge—electron acceptor structure to show facile intramolecular charge transfer and efficient light harvesting ability. Therefore, a π bridge unit should have a good conjugation across a donor and an acceptor for efficient light harvesting and intramolecular charge transfer.

Carbazole is an alternant polycyclic aromatic hydrocarbon consisting of three fused rings with a large, aromatic system, containing nitrogen atom showing extensive electron delocalization. In this paper, four carbazole-based D–π–A dyes were synthesized and used as sensitizers in DSCs. The four dyes were denoted as B-CH, B-C B, DT-CB, and DB-CB, as shown in Scheme 1.

2. Experimental details

2.1. *Materials and characterization*

All chemicals were purchased from Merck and Sigma Aldrich. Solvents and other chemicals are reagent grade and used without further purification. TLC was performed on TLC-Grade silica gel-G/UV 254 nm plates (*n*-hexane, ethyl acetate). Melting points were measured on a Barnstead Electrothermal (BI 9300) apparatus. ^{1}H, ^{13}CNMR spectra were recorded on a FT-NMR Bruker Avanced ultra shield spectrometer (frequency line, 400. MHz for ^{1}HNMR and 100 MHz for ^{13}C NMR; solvents, $CDCl_3$ and DMSO-d_6). Mass spectra of the products were measured with a HP (Agilent Technologies) 5937 Mass Selective Detector. Elemental analyses (C, H, N) were done with a Heraeus CHN-O-Rapid analyzer. FT-IR spectra were recorded in the matrix of KBr with JASCO FT-IR-680 plus spectrometer.

2.2. *Photophysical and electrochemical measurements*

Cyclic voltammetry (CV) studies were performed by biologic SP 150 electrochemical analyzer with scan rate of 100 mVs^{-1} in dimethylformamide containing 0.1 M Bu_4NPF_6 as the supporting electrolyte, platinum wire as counter and work electrodes and Ag/AgCl as reference electrode. The UV–Vis absorbance spectra were measured on a Perkin Elmer (Lambda 25)

spectrophotometer. Current density–voltage measurements were performed using simulated 1.5 AM sunlight with an output power of 100 mW.cm^{-2}. Electrochemical impedance spectroscopy (EIS) was measured in the frequency range of 10^{-1}–10^{5} Hz and in the dark under −0.70V bias. Incident photon-to-current efficiencies (IPCE) were measured with monochromatic incident light of 1×10^{16} photon/cm^2 under 100 mW/cm^{-2} with bias light in DC mode (Jarrel Ash monochromator, using a 100 W halogen lamp) and a calibrated photodiode (Thorlabs) was used to study the optical properties of layers.

2.3. *Fabrication of DSSCs*

The preparation of the photo electrode was performed by application of doctor-blade technique on a conducting glass (FTO, 15 Ω/sq, Dyesol). The paste containing TiO_2 nanoparticles with a diameter of 20 nm (PST-20T, Sharifsolar) was spread on FTO glass. The films were dried at 120°C for 6 min and then sintered at 500°C for 30 min. After sintering the TiO_2 films were immerged into 3×10^{-4}M dyes (DB-CH, DTB-CH, and DT-CH) in acetonitrile/tert-butyl alcohol(1:1; v/v) for overnight. Afterward the dye-covered nanoparticles electrode and Pt-counter electrode were assembled into a sandwich type cell and sealed with 30 μm-thick spacer at 120°C for a few seconds. After the injection of the electrolyte solution, which consists of 0.5 M LiI, 0.05 M I_2, and 0.1 M 4-tert-butylpyridine in acetonitrile into the interspace between the photo anode and the counter electrode, the photo electrochemical property of the DSSC was measured.

2.4. *Computational methods*

The optimization of the geometries of B-CH, B-C B, DT-CB, and DB-CB have been done by using the B3LYP method with the 6–31 G (d) basis set. Density functional theory (DFT) calculations of dyes were performed by Gaussian 03 package.

2.5. *Synthesis of dyes*

2.5.1. *Synthesis of 9-Butyl-9H-carbazole*

To a stirred solution of carbazole (0.2 g, 1.1 mmol) in DMSO (3 mL), NaOH (0.4 g) was added and then the corresponding *n*-butylbromide (0.137 g, 1.01 mmol) was added drop wise. After complete addition, the reaction mixture was heated at 90°C overnight. The organic layer was separated, washed with water, dried over Na_2SO_4 and concentrated. Pure product was obtained after silica gel column chromatography (normal hexane) as a white solid.

White powder, Yield: 83%, mp: 54–55°C

^{1}HNMR (300 MHz, $CDCl_3$): 8.22 (m, 2H), 7.55 (m, 4H), 7.35 (m, 2H), 4.42 (t, $J = 6.3$ Hz, 2H), 1.98 (m, 2H), 1.52 (m, 2H), 1.06 (t, $J = 7.2$ Hz, 3H) ppm.

FT-IR (cm^{-1}): 3043, 2953, 2928, 1918, 1625, 1591, 1482, 1463, 1348, 1325.

2.5.2. *Synthesis of 9-Hexyl-9H-carbazole*

To a stirred solution of carbazole (0.2 g, 1.1 mmol) in DMSO (3 mL), NaOH (0.4 g) was added. Then the corresponding hexylbromide (0.335 g, 1.01 mmol) was added dropwise. After complete addition, the reaction mixture was heated at 90°C overnight. The organic layer was separated, washed with water, dried over Na_2SO_4 and concentrated. Pure product was obtained after silica gel column chromatography (normal hexane) as a white solid.

White powder, yield: 85%, mp: 75–77°C

^{1}HNMR (400 MHz, $CDCl_3$) δ (ppm): 0.87 (t, $J = 7.043$ Hz, 3H), 1.26–1.43 (m, 6H), 1.87 (m, 2H), 4.30 (t, $J = 7.043$ Hz, 2H), 7.22 (t, $J = 7.825$ Hz, 2H), 7.40–7.48 (m, 4H), 8.09 (d, $J = 7.825$ Hz, 2H)

^{13}CNMR (100 MHz, $CDCl_3$) δ (ppm): 14.6, 23.1, 27.5, 29.4, 32.1, 43.4, 109.2, 119.2, 120.9, 123.3, 126.1, and 140.9

IR (cm^{-1}): 3051, 2955, 2923, 2869, 2856, 1628, 1594, 1487, 1453, 1376, 1327, 1241, 1217, 1192, 1153, and 1128

2.5.3. *9-Butyl-9H-carbazole-3-carbaldehyde(2)*

Phosphorylchloride (1.55 mL, 1.25 eq) was added drop wise to N, N-dimethylformamide (DMF, 0.88 mL, 1.15 eq) for 1 h at 0°C. The mixture was stirred and then N-(butyl) carbazole (0.25 g, 1 mmol) added over 1 h at room temperature. After standing for 5 hr at 90°C, the mixture was poured into ice–water (30 mL), stirred 5 hr, and neutralized with sodium hydroxide. The solution was extracted three times with ethyl acetate and dried with Na_2SO_4. The solvent was removed under reduced pressure. The residue was purified by silica gel column chromatography (eluent: ethyl acetate/*n*-hexane = 1:9).

Cream powder, Yield: 55%, mp: 62–64°C

^{1}HNMR (DMSO-d_6, 400 MHz) δ (ppm): 10.06 (s, 1H), 8.76 (s, 1H), 8.30 (d, $J = 8$ Hz, 1H), 7.99 (m, 1H), 7.79 (d, $J = 8$ Hz, 1H), 7.70 (d, $J = 8$ Hz, 1H), 7.54 (m, 1H), 7.31 (t, $J = 7.6$ Hz, 1H), 4.46 (t, $J = 8$ Hz, 2H), 1.76 (m, 2H),1.29 (m, 2H), and 0.87 (t, $J = 8$ Hz, 3H)

^{13}CNMR (DMSO-d_6, 100 MHz) δ (ppm): 191.8, 143.4, 140.8, 128.2, 126.4, 124, 122.1, 120.8, 120.40, 110, 109.8, 42.2, 30.6, 19.8, and 13.8

FT-IR (cm^{-1}): 2985, 1691, 1625, 1594, 1473, 1352, 1133, and 808

2.5.4. *9-Hexyl-9H-carbazole-3-carbaldehyde)3)*

Phosphorylchloride (1.55 mL, 1.25 eq) was added drop wise to DMF (0.88 mL, 1.15 eq) for 1 hr at 0°C. The mixture was stirred and then N-(hexyl) carbazole (0.25 g, 1 mmol) added over 1 hr at room temperature. After standing for 5 hr at 90°C, the mixture was poured into ice–water (30 mL), stirred 5 hr, and neutralized with sodium hydroxide. The solution was extracted three times with ethyl acetate and dried with $MgSO_4$. The solvent was removed under reduced pressure. The residue was purified by silica gel column chromatography (eluent: ethyl acetate/*n*-hexane = 1:9).

Cream powder, Yield: 55%, mp: 70–74°C

^{1}HNMR (DMSO-d_6, 400 MHz) δ (ppm): 10.06 (s, 1H), 8.77 (s, 1H), 8.30 (d, $J = 8$ Hz, 1H), 7.79 (d, $J = 8$Hz, 1H), 7.70 (m, 1H), 7.55 (m, 1H), 7.31 (t, 8Hz, 1H), 4.46 (t, $J = 8$ Hz, 2H), 1.77 (m, 2H), 1.25 (m, 6H), and 0.87 (t, $J = 8$ Hz, 3H)

^{13}CNMR (DMSO-d_6, 100 MHz) δ (ppm): 13.7, 22, 26, 28.4, 30.9, 42.5, 109.7, 110.2, 120, 120.7, 122.11, 122.2, 124, 126.6, 126.7, 128.2, 140.4, 142.6, and 192

IR (cm^{-1}): 3052, 2955, 2929, 2857, 2727, 1893, 1686, 1593, 1469, 1383, 1352, 1339, 1329, 1240, 1177, 1135, 807, 765, 748, and 730.

2.5.5. *Synthesis of butyl-carbazole-3,6-dicarbaldehyde (1)*

Phosphorylchloride (2.31 mL, 2.5 eq) was added drop wise to DMF (1.76 mL, 2.3 eq) for 1 hr at 0°C. The mixture was stirred and then N-(butyl) carbazole (0.22 g, 1 mmol) added over 1 hr at room temperature. After standing for overnight at 90°C, the mixture was poured into ice–water (30 mL), stirred 5 hr, and neutralized with sodium hydroxide. The solution was extracted three times with ethyl acetate and dried with $MgSO_4$. The solvent was removed

under reduced pressure. The residue was purified by silica gel column chromatography (eluent: ethyl acetate/*n*-hexane = 1:9).

Cream powder, Yield: 60%, mp: 145–150°C

^{1}HNMR (DMSO-d_6, 400 MHz) δ (ppm): 10.9 (s, 2H), 8.87 (s, 2H), 8.77 (d, $J = 8$ Hz, 2H), 8.08 (d, $J = 8$ Hz, 2H), 4.50 (t, $J = 12$ Hz, 2H), 1.75 (m, 2H), 1.30 (m, 2H) and 0.87 (t, $J = 1.11$ Hz, 3H)

^{13}CNMR (DMSO-d_6, 100 MHz) δ (ppm): 191.9, 144.3, 129.3, 127.3, 124.5, 122.2, 110.7, 42.7, 30.6, 19.7 and 13.6

FT-IR (cm^{-1}): 2956, 2863, 2811, 2722, 1685, 1629, 1627, 1592, 1488, 1205 and 1125

2.5.6. *Synthesis of 5-[9-butyl-6-(2,4-dioxo-1,3-thiazolan-5-ylidenmethyl)-9H-3-carbazolyl]methylidene-1,3-thiazolane-2,4-dione) DT-CB)*

Butyl-carbazole-3,6-dicarbaldehyde (0.31 g, 1 mmol) and thiazolidine-2,4-dione (0.23 g, 2 mmol) and ammonium acetate (0.15 g, 1.9 mmol) were dissolved in acetic acid (2 mL). The reaction mixture was refluxed for 5 hr. The orange crystals thus obtained were filtered, washed with excess water three times. The dye BD-CH obtained was purified by crystallization from EtOAc/n-hexane.

Orange, Yield: 63%

^{1}HNMR (DMSO-d_6, 400 MHz) δ (ppm): 12.50 (s, 2H), 8.76 (s, 2H), 8.40 (s, 2H), 7.89 (s, 2H), 7.64 (d, $J = 4$ Hz,2H), 7.61 (d, $J = 4$ Hz, 2H), 4.36 (t, $J = 6$ Hz, 2H), 1.73 (m, 2H), 1.26 (m, 2H) and 0.86(t, $J = 8$ Hz, 3H)

^{13}CNMR (DMSO-d_6, 100 MHz) δ (ppm): 168, 167.5, 141.3, 132.8, 128.3, 124.6, 123.4, 122.4, 119.8, 110.6, 42.5, 30.6, 19.7, and 13.6

Mass: *m/z* 478 (M+1), 477, 434, 406, and 376

FT-IR (cm^{-1}): 3433, 3117, 2959, 2771, 1734, 1683, 1629, 1583, 1488, 1458, 1432, 1388, 1321, 1295, 1276, 1251, and 1213

Anal. Calcd for C24H19N3O4S2 (477.08): C, 60.37; H, 4.01; N, 8.80 Found: C, 60.42; H, 4.0 6; N, 8.90

2.5.7. *Synthesis of 5-[9-butyl-6-(2,4,6-trioxohexahydro-5-pyrimidinylidenmethyl)-9H-3-carbazolylmethylene]hexahydro-2,4,6-pyrimidinetrione (DB-CB)*

Butyl-carbazole-3,6-dicarbaldehyde (0.31 g, 1 mmol), and barbutiric acid (0.29 g, 2 mmol) were dissolved in absolute ethanol (3 mL). The reaction mixture was refluxed for 5 hr. The dark orange crystals thus obtained were filtered, washed with excess water three times. The dye BTD-CB obtained was purified by crystallization from EtOAc/n-hexane.

Dark orange, Yield: 87%

^{1}HNMR (DMSO-d_6, 400 MHz) δ (ppm): 11.35 (s, 2H), 11.25 (s, 2H), 9.25 (s, 2H), 8.46 (s, 2H), 8.40 (d, $J = 8$, 2H), 7. 70 (d, $J = 8$ Hz, 2H), 4.40 (t, $J = 6$, 2H), 1.74 (m, 2H), 1.28 (m, 2H), and 0.8 (t, $J = 8$, 3H)

^{13}CNMR (DMSO-d_6, 100 MHz) δ (ppm): 164.0, 162.5, 160.08, 155.3, 150.3, 143.6, 134.3, 128.3, 124.7, 122.3, 115.1, 109.1, 42.7, 30.6, 19.7, and 13.6

Mass: *m/z* 501 (M+1), 499, 487, 481, 453, and 431

FT-IR (cm^{-1}): 3417, 3201, 3065, 2957, 2930, 2854, 1740, 1734, 1667, 1492, 1531, 1483, 1440, 1402, 1377, 1309, 1241, and 1197

Anal. Calcd for C26H21N5O6 (499.47): C, 62.52; H, 4.24; N, 14.02 Found: C, 62.61; H, 4.33; N, 15.51.

2.5.8. *Synthesis of 5-(9-Butyl-9H-carbazol-3-ylmethylene)-pyrimidine-2, 4, 6-trione (B-CB)*

Butyl-carbazole-3-carbaldehyde (0.25 g, 1 mmol), and barbutiric acid (0.15 g, 1 mmol) were dissolved in absolute ethanol (3 mL). The reaction mixture was refluxed for 5 h. The orange crystals thus obtained were filtered, washed with excess water three times. The dye B-CB obtained was purified by crystallization from EtOAcn-hexane.

Orange, Yield: 78%

^{1}HNMR (DMSO-d_6, 400 MHz) δ (ppm): 11.33(s, 1H), 11.20(s, 1H), 9.30(s, 1H), 8.64(d, $J = 8$, 2H), 8.53(s, 1H), 8.18 (d, $J = 8$, 2H), 7.71 (t, $J = 10$, 1H), 7.54 (m, 2H), 7.32 (t, $J = 8$, 1H), 4.45 (t, $J = 12$, 2H), 1.76 (m, 2H), 1.30 (m, 2H), and 0.88 (t, $J = 8$, 3H)

^{13}CNMR (DMSO-d_6, 100 MHz) δ (ppm): 164. 2, 162.4, 156.9, 150.2, 143.1, 140.7, 133.3, 129.5, 126.7, 123.4, 122.4, 122.1, 120.3, 120.5, 114.0, 110.3, 109.3, 42.4, 30.6, 19.7, and 13.7

Mass: *m/z* 361.4 (M+1), 362, 361, 318, 261, and 204

FT-IR (cm^{-1}): 3852, 3841, 3742, 3687, 3674, 3648, 3618, 3437, 3189, 3060, 2957, 2862, 1669, 1539, 1740, and 1401

Anal. Calcd for C21H19N3O3 (361.4): C, 69.79; H, 5.30; N, 11.63 Found: C, 69.9; H, 5.57; N, 11.65

2.5.9. *Synthesis of 5-(9-Hexyl-9H-carbazol-3-ylmethylene)-pyrimidine-2, 4, 6-trione (B-CH)*

Hexyl-carbazole-3-carbaldehyde (0.27 g, 1 mmol), and bituric acid (0.15 g, 1 mmol) were dissolved in absolute ethanol (3 mL). The reaction mixture was refluxed for 5 hr. The orange crystals thus obtained were filtered, washed with excess water three times. The dye B-CB obtained was purified by crystallization from EtOAc/n-hexane.

Orange, Yield: 82%

^{1}HNMR (DMSO-d_6, 400 MHz) δ (ppm): 11.32 (s, 1H), 11.20 (s, 1H), 9.30 (s, 1H), 8.60 (d, $J = 8$, 2H), 8.16 (s, 1H), 7.70 (d, $J = 8$, 2H), 7.54 (t, $J = 10$, 1H), 7.30 (m, 2H), 7.32 (t, $J = 8$, 1H),4.45 (t, $J = 6$, 2H), 3.36 (m, 2H), 2.51 (m, 2H), 1.77 (m, 2H), 1.24 (m, 2H), and 0.78 (t, $J = 8$, 3H)

^{13}CNMR (DMSO-d_6, 100 MHz): 164.2, 162.4, 156.9, 150.2, 143.1, 140.6, 133.4, 129.5, 126.7, 123.5, 122.4, 122.1, 120.6, 120.4, 114.0, 110.3, 109.2, 42.6, 30.9, 28.5, 26.0, 22.0, and 13.7

Mass: *m/z* 390 (M+1), 389, 318 and 204

FT-IR (cm^{-1}): 3901, 3826, 3744, 3423, 3190, 3059, 2954, 2921, 2855, 1692, 1523, 1464, 1401, and 1146

Anal. Calcd for C23H23N3O3 (389.17): C, 70.93; H, 5. 95; N, 10.79 Found: C, 70.99; H, 6.07; N, 10.89

3. *Results and discussion*

3.1. *Synthesis and characterization*

The molecular structures and synthetic routes of the four organic dyes B-CH, B-C B, DT-CB, and DB-CB are represented in Schemes 1 and 2, respectively. All of the dyes have been synthesized by the stepwise synthetic protocol. Every dye contains three essential parts include π donor, linker and π acceptor. Carbazole is an aromatic hydrocarbon chose as linker. In order to investigate the effect of π donor and π acceptor on the dye performances, two donor units include butyl and hexyl and barbutiric acid and thiazolidine-2,4-dione were applied as acceptor. Firstly, hexyl and butyl moieties were introduced to carbazole by the reaction in

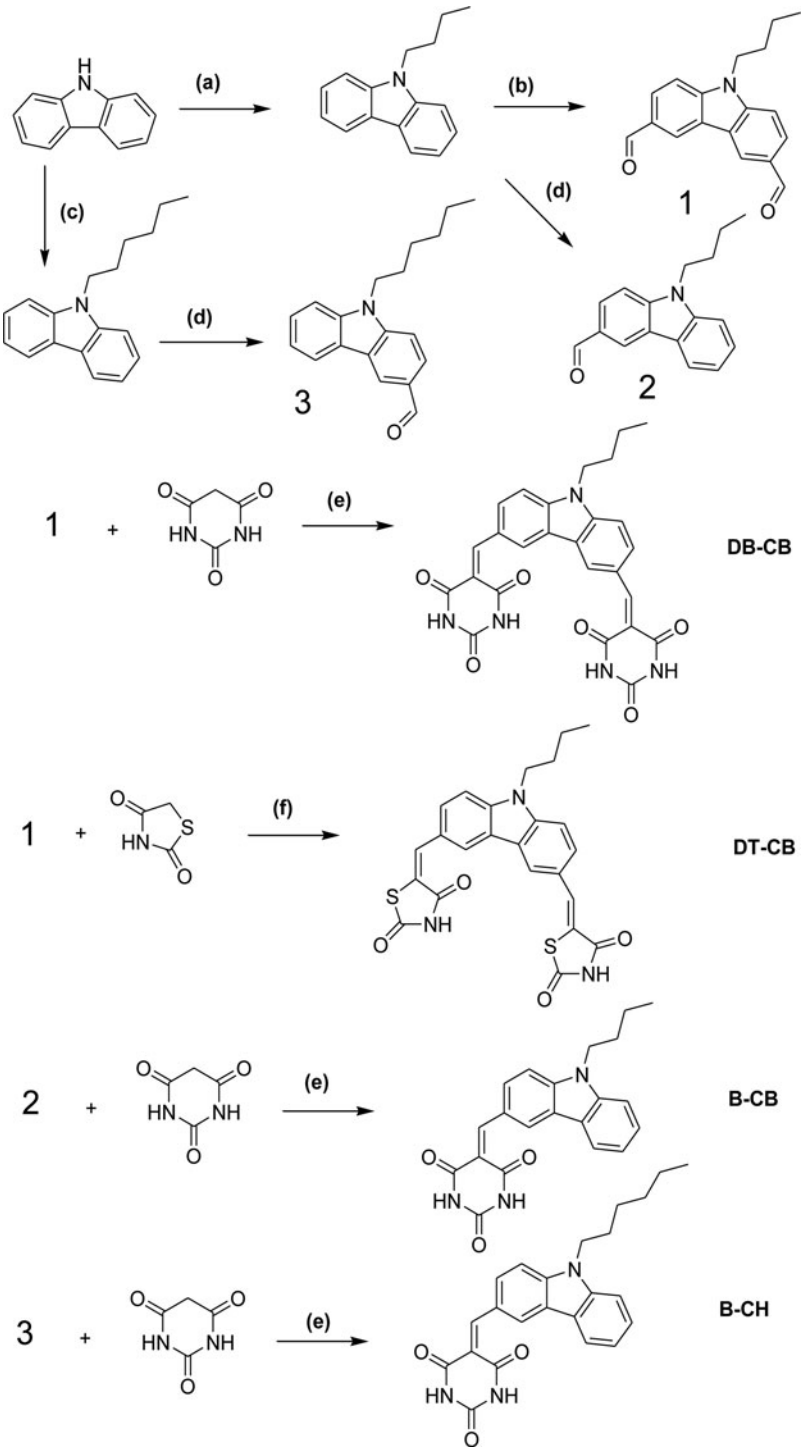

Scheme 2. Synthetic routes of DB-CH, DTB-CH, and DT-CH (a) 1-Bromohexyl, NaOH, DMSO, 110°C, overnight (b) POCl3, DMF, 95°C, overnight (c) 1-Bromobutyl, NaOH, DMSO, 110°C, overnight (d) POCl3, DMF, 95°C, 5 hr (e) Ethanol, 55°C, 5 hr (f) Acetic acid, Amonium acetate, 90°C, 10 hr.

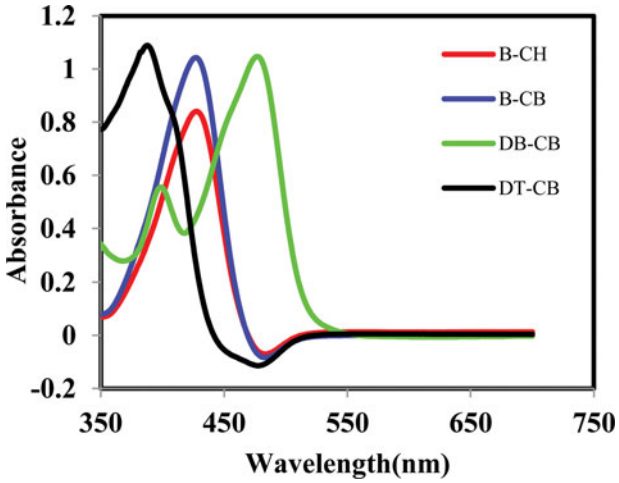

Figure 1. Absorption spectra of dyes B-CH, B-C B, DT-CB, and DB-CB in THF.

the presences of NaOH and DMSO as solvent. The role of alkyl unit in addition of donor, decrease aggregation of dyes in TiO_2 surface and fulfill better dye efficiency. In the next step 9-alkyl-9H-carbazole undergoes Vilsmeier–Haack reaction for formylation. In order depicted in Scheme 2, 9-butyl-9H-carbazole dose Vilsmeier–Haack reaction in one and two sides. Nevertheless, 9-Hexyl-9H-carbazole was subjected to mono aldehyde. In final synthetic protocol different precursors 1, 2, and 3 were used for preparation of dyes. In this step, active methylene such as barbutiric acid as six-member ring and thiazolidine-2,4-dione as five-member ring react by formylated precursors by Knoevenagel condensation. The overall yield for final step was (63%–85%).

3.2. *UV–Vis absorption spectra*

The ultraviolet–visible (UV–Vis) absorption spectra of the four dyes in diluted THF solution (3×10^{-4} M) are presented in Fig. 1, and the corresponding data are collated in Table 1. All dyes except DB-CB showed one broad peak in region (350–540) nm. The DB-CB showed two

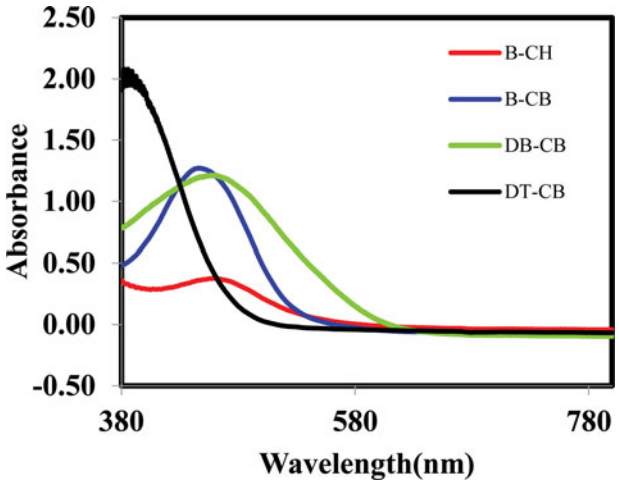

Figure 2. Absorption spectral of dyes B-CH, B-C B, DT-CB, and DB-CB on TiO_2 film.

peaks in 379 and 474 nm. It is notable absorption band is in the UV region (300–370 nm) corresponding to the $\pi-\pi/$ electron transitions of the conjugated molecules; and the other is in the visible region (400–550 nm) that can be assigned to an intramolecular charge transfer (ICT). The three other dyes show peak in λ_{max} of 427,426 and 387 for B-CH, B-CB and DT-CB respectively. The λ_{max} of B-CH and B-CB correspond to visible region but the λ_{max} of DT-CB correspond to UV region. These differences attributed to their structure, both of B-CH, B-CB have one barbutiric acid as acceptor unit. DB-CB has two barbutiric acids as acceptor unit. However, DT-CB contains two five member ring thiazolidine-2, 4-dione as acceptor.

In order to study the absorption of dyes in TiO_2 surface, absorption spectral of dyes B-CH, B-C B, DT-CB and DB-CB on TiO_2 film is displayed in Fig. 2. All dyes showed one broad peak in the range of 380–600 nm. The λ_{max} for B-CH, B-CB, DT-CB, and DB-CB is 459, 439.5, 381, and 453 nm, respectively. Roughly all dyes show red shift in the range of 6–32 nm with respect to those in solutions. It is presumed that the red and blue shifts of the absorption spectra may be contributed to the formation of aggregates on the TiO_2 surface [14,28]. Therefore, B-CH due to having longer alkyl group shows less aggregation. Other obvious phenomena in absorption of dyes in TiO_2 surface related to threshold of spectral. Higher threshold in absorption of dyes on TiO_2 surface attributed to higher aggregations. By the way, DT-CB shows shorter threshold and most absorption on TiO_2 surface. These results indicate in addition of donor unit, acceptor unite play important role in absorption and aggregation phenomenon because DT-CB despite having lower alkyl unit shows less aggregation. Also it may be attributed to different function of anchoring groups. Their function may be differing in solution and anchored to TiO_2 molecules.

3.3. *Electrochemical properties*

In order to evaluate the possibilities of electron transfer from the excited states of B-CH, B-C B, DT-CB, and DB-CB to the conduction band of TiO_2 and regeneration of the dyes, cyclic voltammetry was applied to investigate the redox behavior (Fig. 3) and related information are presented in Table 1.

The HOMO levels of dyes B-CH, B-C B, DB-CB, and DT-CB is 1.03, 1.09, 1.02, and 1.03 V (vs. NHE), respectively. All dyes have near HOMO levels, but all are satisfactory in due to be

Table 1. UV-Vis and electrochemical data.

Dye	B-CH	B-CB	DB-CB	DT-CB
UV(λ_{max}/nm)[a]	459	439.5	453	381
UV(λ_{max}/nm)[a]	427	427	477	388
Reduction(V vs. NHE)[b]	− 1.56	−1.43	−1.34	−1.72
Oxidation(V vs. NHE)[c]	1.03	1.09	1.02	1.03
E0–0[d]	2.59	2.57	2.36	2.75
HOMO/LUMO (ev)[f]	−6.71/−9.02	−6.71/−9.02	−6.83/−9.01	−6.31/−8.18
Band gap (ev)[f]	2.31	2.31	2.18	1.87

[a]Maximum absorption on TiO_2 film.
[b]Maximum absorption in THF.
[c]Oxidation of dyes measured by cyclic voltametery in 0.1 M Bu4NPF6 in THF solution as supporting electrolyte, Ag/AgCl as reference electrode and Pt as counter electrode. Potentials measured vs Ag/AgCl was converted to normal hydrogen electrode (NHE) by addition of +0.2V[48]
[d]Reduction was calculated by HOMO–E0–0.
[e]E0–0 transition energy measured at the onset of absorption spectra.
[f]DFT/B3LYP calculated values.

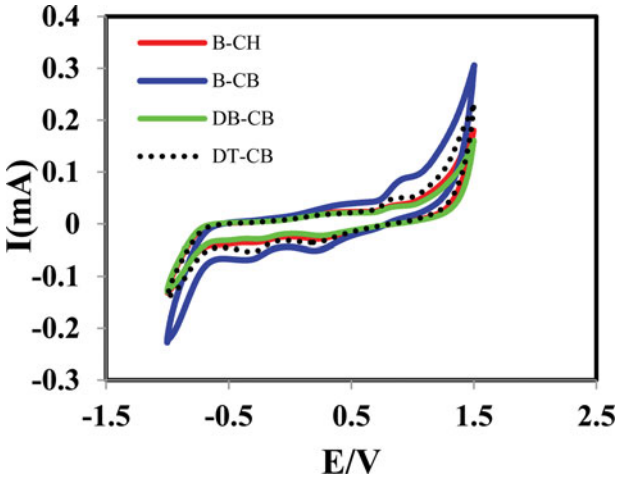

Figure 3. CVs of the B-CH, B-C B, DT-CB, and DB-CB dye films in DMF containing 0.1 M Bu4NPF6 at a scan rate of 100 mVs^{-1}, vs Ag/AgCl.

more positive than the iodine/iodide redox potential value (0.4v) vs. NHE. These values indicate all dyes fulfill efficient regeneration of dye cation after photo induced electron injection in to TiO_2 film. The LUMO levels of dyes B-CH, B-C B, DB-CB, and DT-CB is −1.56, −1.43, −1.34, and −1.72 V (vs. NHE), respectively. These values are more negative than TiO_2 conduction band edge (−0.5 vs NHE). Therefore, ensure electron injection from the excited dye in to the conduction band of TiO_2. E 0–0 transition energy measured at the onset of absorption spectra. The difference in band gap originates from different structural units spatially acceptor unit. DT-CB has the most band gap, 2.75 and other dyes have near band gap. E0–0 is 2.59, 2.57, and 2.36 for B-CH, B-C B, and DB-CB, respectively. Potentials measured vs. Ag/AgCl was converted to normal hydrogen electrode (NHE) by addition of +0.2V. The schematic energy levels of B-CH, B-C B, DT-CB, and DB-CB based on absorption and electrochemical data are shown in Fig. 4.

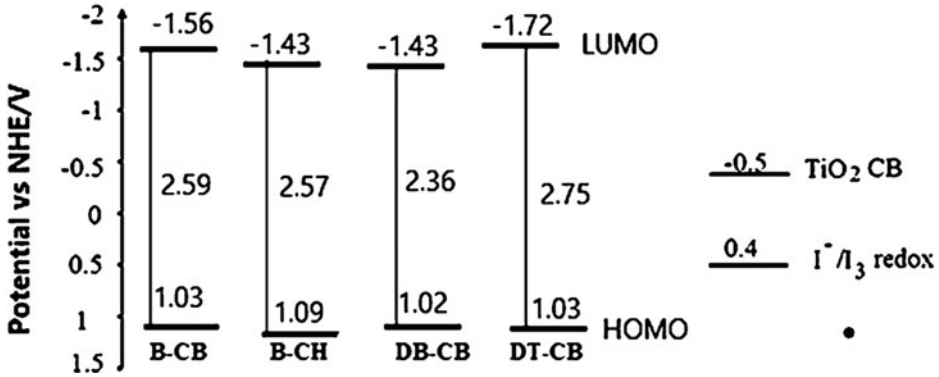

Figure 4. Schematic energy levels of B-CH, B-C B, DT-CB, and DB-CB based on absorption and electrochemical data.

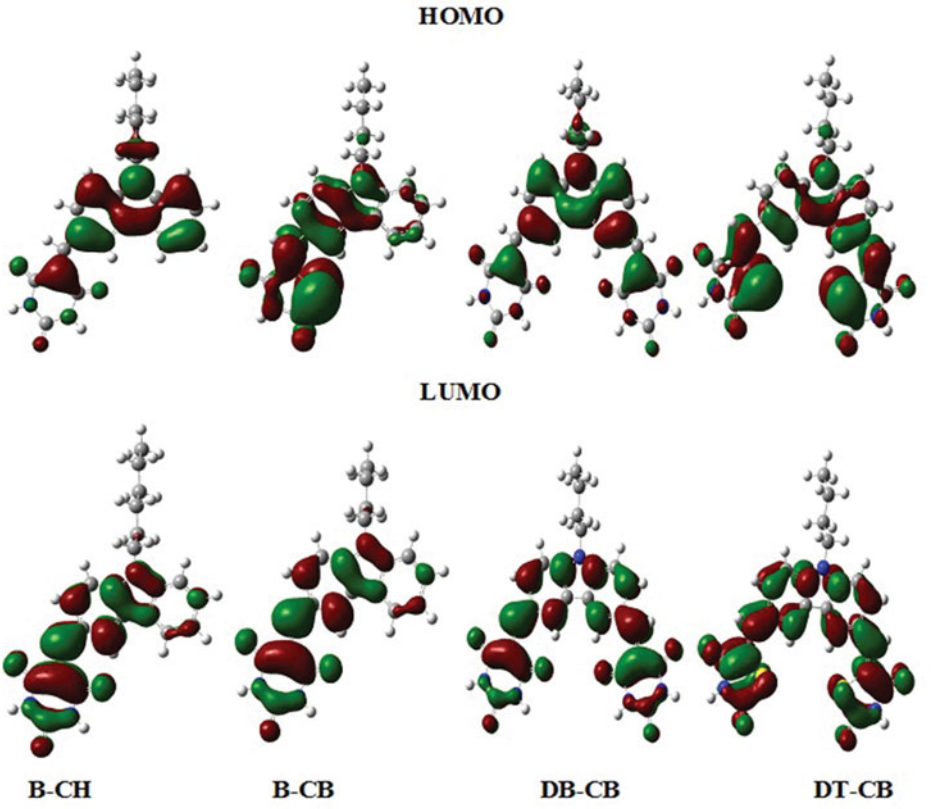

Figure 5. The electron distribution of the HOMO and LUMO of B-CH, B-C B, DT-CB, and DB-CB.

3.4. *Theoretical calculation*

To visualize and gain further insight into the results from cyclic voltammetry, density function theory (DFT) calculations were carried out by the B3LYP/6-31G (d) levels. Electron distributions of HOMO and LUMO level of dyes is shown in Fig. 5. In HOMO level dyes don't show similar electron distribution. Electrons in CB-H are located in carbazole and first CH2 of hexyl

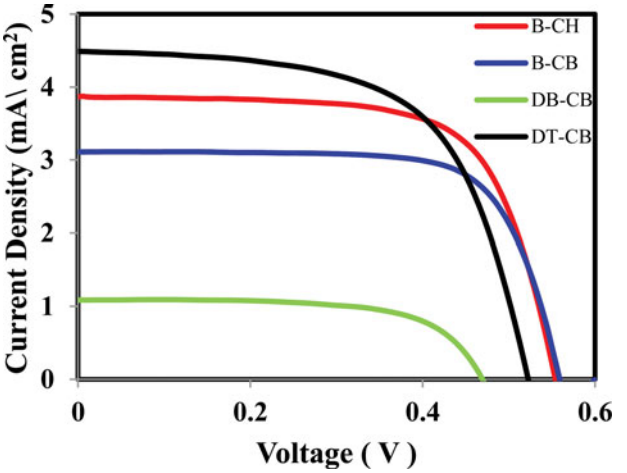

Figure 6. J–V characteristics of cells with different dyes as sensitizer.

Table 2. Photovoltaic parameters for cells.

	B-CH	B-CB	DB-CB	DT-CB
J_{SC} (mA.cm^{-2})	3.87	3.11	1.08	4.48
V_{OC} (V)	0.55	0.56	0.47	0.52
FF	68	72	65	61
η (%)	1.47	1.26	0.33	1.44

and upper side of barbutiric acid, for CB-B in addition of carbazole total ring of barbutiric acid contain electron distribution. DB-CB is similar to CB-H but contain both of barbutiric rings. Electron distribute all over carbazole and acceptor units in DT-CH. The electrons locate similarly in LUMO level. Two dyes B-CH and B-CB have the same distribution over the some part of carbazole and barbutiric acid. In addition, DB-CB and DT-CB have comparable electron distribution in all over carbazole and two acceptor units.

3.5. *Photovoltaic properties*

Figure 6 shows the current density–voltage (J–V) curves of the cells with different dyes as sensitizer under AM 1.5 light illumination. The photoelectrode chemical properties of these cells are listed in Table 2; FF, VOC, and JSC are fill factor, open circuit photovoltage, and short-circuit photocurrent, respectively. We obtained a solar energy to electricity conversion efficiency of 1.47% (Jsc = 3.87 mA cm^{-2}, Voc = 0.55V, FF = 0.68), 1.26% (Jsc = 3.11 mA cm^{-2}, Voc = 0.56V, FF = 0.72), 1.44% (Jsc = 4.48 mA cm^{-2},Voc = 0.52V, FF = 0.61) and 0.33% (Jsc = 1.08 mA cm^{-2},Voc = 0.47 mV, FF = 0.65) with DSCs-based B-CH, B-CB, DT-CB, and DB-CB, respectively. For the DT-CB & B-CH dye, cells have better performance compared to other dyes. A larger Voc and Jsc are a prerequisite for higher power conversion efficiencies in DSCs. The increased Jsc value of DT-CB compared with other three dyes mainly derived from its relatively better light harvesting ability reflecting in its better IPCE spectrum. The increased energy to electricity conversion efficiency of B-CH compare to DT-CB is related to higher Voc.

Incident photon-to-electron conversion efficiency (IPCE) spectra of the cells are shown in Fig. 7. The IPCE curves of DSSCs based on B-CH, B-CB, DT-CB, and DB-CB exhibited broad

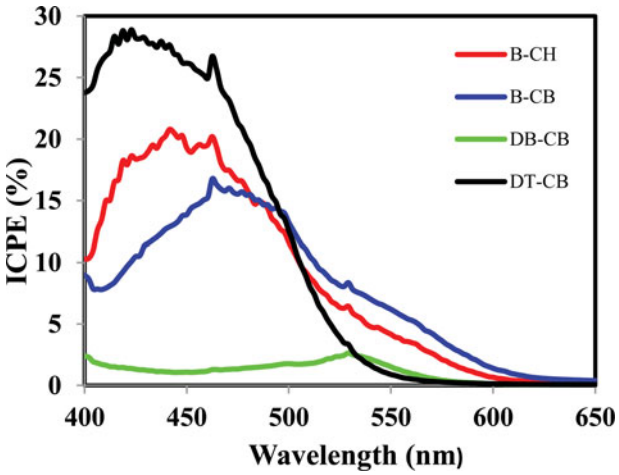

Figure 7. IPCE spectra of cells.

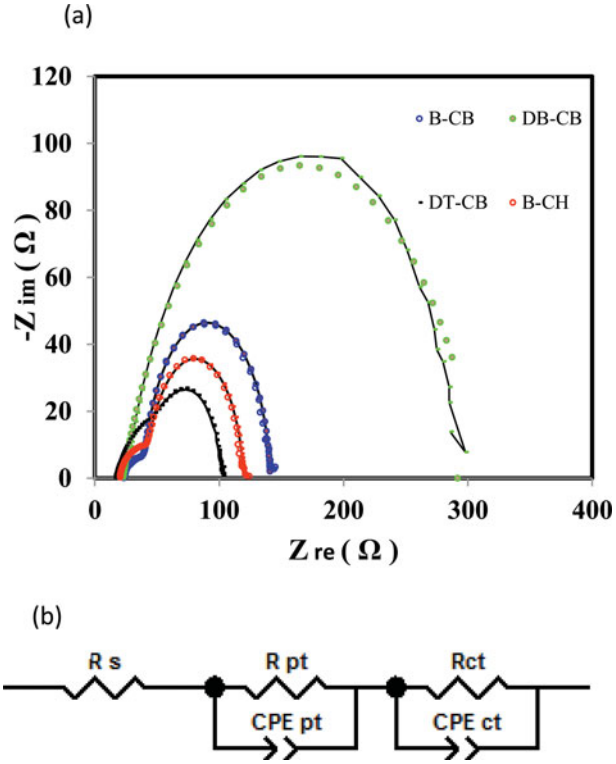

Figure 8. (a) EIS spectra of cells, (b) equivalent circuit for (a).

absorption in the range of 400–650 nm, with maxima at 19.9, 16.8, 28.4, and 3.5%, respectively. There is no consistent with the absorption spectra in Fig. 2 and ICPE of the DB-CH. This malfunction may be attributed to two barbutiric acids in structure of DB-CB. Actually one of barbutiric acids has different spatial orientation. Therefore it cannot anchor to TiO_2 molecules. It withdraw the electron population on itself and decrees electron population on other barbutiric acid anchor to TiO_2 molecules. Therefore DB-CH cannot act properly as a (D–π–A) organic dye. Roughly other dyes are consistent with the absorption spectra in solution and ICPE. In comparison with dyes B-CH gives the higher IPCE value, which implies the dye would show a relatively large photocurrent in DSSCs [49]. It is obvious that the DT-CB dye as sensitizer in cells show higher IPCE which is in a good agreement with the results of J-V characterization. The B-CH & DT-CB have higher IPCE in higher wavelengths.

To investigate the charge recombination in the DSSCs based on the four dyes, EIS spectra dyes measured in the dark under −0.70V bias. Fig. 8 (a) shows the electrochemical impedance spectroscopic (EIS) analysis of the cells and equivalent circuit is represented in Fig. 8 (b). The larger semicircle at lower frequencies corresponded to the charge transfer processes at the TiO_2/dye/electrolyte interface, while the smaller semicircle at higher frequencies corresponded to the charge transfer processes at the Pt/electrolyte interface. The results of EIS data fits listed in Table 3. R_{ct}, τ and C_μ correspond to the charge transfer process occurring at the TiO_2/dye/electrolyte interface, electron life time and chemical capacitance, respectively. CPE ct-T and CPE ct-P are parameters of constant phase elements charge transfer (CPE ct). Important parameters form DSSCs, electron lifetime (τ), are extracted from the (C_μ) and R_{ct} using $\tau = C_\mu \times R_{ct}$. Radius of the larger semicircle in the Nyquist plot decreased in the following order: DB-CB > B-CB > B-CH > DT-CB indicating that DT-CB and DT-CB have

Table 3. EIS parameters obtained from modeling the EIS result.

	R_{ct} ($\Omega.cm^2$)	CPE ct-T (10−4)	CPE ct-P	τ (ms)	C_{μ} ($10^2 \mu F.cm^{-2}$)
B-CH	18.29	2.63	0.97	16.80	9.18
B-CB	24.57	3.03	0.96	25.49	10.38
DB-CB	69.12	1.04	0.77	9.98	1.44
DT-CB	15.96	3.12	0.80	7.46	4.67

more efficient electron transportation at the TiO_2/dye/electrolyte interface. In comparison of smaller semicircle, DT-CB has bigger radius. This phenomenon shed out the little deficiency of DT-CB in comparison to DT-CB. This dye has less efficient electron transportation at the Pt/electrolyte interface. According to J-V curve results, the cell prepared with B-CH dye has the largest efficiency. The EIS spectra analysis proves this claim and the R_{ct} value is low, too.

4. Conclusion

Four metal-free organic dyes comprising a carbazole linker and butyl and hexyl as the common electron donor and novel anchoring group, active methylene such as barbutiric acid as six member ring and thiazolidine-2,4-dione as five member ring were designed and synthesized for investigation in dye-sensitized solar cells (DSSCs). Actually, effect of two electron donor and electron acceptor on the efficiency of sensitizer was studied. Hexyl and butyl chose for overcome the obstacle of aggregation and evaluate the effect of length of alkyl on this phenomenon. Result indicates dye contain hexyl show better overall efficiency (η (%): 1.47). In order to study anchoring group effect two dyes DT-CB and DB-CB by same donor unit evaluated. DT-CB by thiazolidine-2,4-dione as five member ring has better performance and overall of its efficiency was (η (%): 1.44). It is notable to understand the effect of number of anchoring group DB-CB and B-CB can be compare. It is clear B-CB by the efficiency of (η (%): 1.26) is more suitable for application in dye-sensitized solar cells.

Acknowledgment

We are grateful to the Yasouj University and industrial Sharif University.

References

[1] Graetzel, M. (2001). *Nature*, *414*, 338.
[2] Hagfeldt, A., Boschloo, G., Sun, L., Kloo, L., & Pettersson, H. (2010). *Chem. Rev.*, *110*, 6595.
[3] Choi, J., et al. (2014). *Mol. Cryst. Liq. Cryst.*, *600*, 22.
[4] Han, L. et al. (2014). *J. Photochem. Photobiol. A*, *290*, 54–62.
[5] Jung, M. et al. (2013). *Mol. Cryst. Liq. Cryst.*, *586*, 111.
[6] Stathatose, E. (2014). *J. Photochem. Photobiol. A*, *294*, 54.
[7] Mishra, A., Fischer, M. K. R., & Bauerle, P. (2009). *Angew. Chem. Int. Ed.*, *48*, 2474.
[8] Zhu, W. et al. (2011). *Adv. Funct. Mater.*, *21*, 756.
[9] Bredas, J. L., Norton, J. E., Cornil, J., & Coropceanu, V. (2009). *Acc. Chem. Res.*, *42*, 1691.
[10] Chang, Y. J., & Chow, T. J. (2011). *J. Mater. Chem.*, *21*, 9523.
[11] He, J.et al. (2011). *J. Mater. Chem.*, *21*, 6054.
[12] Mathew, S., & Imahori, H. (2011). *J. Mater. Chem.*, *21*, 7166.
[13] Cai, N. et al. (2011). *Nano Lett.*, *11*, 1452.
[14] Yella, A. et al. (2011). *Science*, *334*, 629.
[15] Ning, Z., Fu, Y., & Tian, H. (2010). *Energy Environ. Sci.*, *3*, 1170.

[16] Nazeeruddin, M. K., Pechy, P., Renouard, T., Zakeeruddin, S. M., & Humphry-Bake, R. (2001). *J. Am. Chem. Soc.*, *123*, 1613.
[17] Hara, K. et al. (2001). *Chem. Commun.*, *6*, 569.
[18] Hara, K. et al. (2005). *J. Phys. Chem. B*, *109*, 15476.
[19] Wang, Z. S. et al. (2007). *Adv. Mater.*, *19*, 1138.
[20] Wu, W., Hua, J., Jin, Y., Zhan, W., & Tian, H. (2008). *Photochem. Photobiol. Sci.*, *7*, 63.
[21] Horiuchi, T., Miura, H., & Uchida, S. (2003). *Chem. Commun.*, *24*, 3036.
[22] Zhu, W. et al. (2011). *Adv. Funct. Mater.*, *21*, 756.
[23] Shibano, Y., Umeyama, T., Matano, Y., & Imahori, H. (2007). *Org. Lett.*, *9*, 1971.
[24] Wang, Z., Li, F., & Huang, C. (2000). *Chem. Commun.*, *20*, 206.
[25] Velusamy, M., Thomas, K. R. J., Lin, J. T., Hsu, Y. C., & Ho, K. C. (2005). *Org. Lett.*, *7*, 1902.
[26] Kim, S. et al. (2006). *J. Am. Chem. Soc.*, *128*, 16701.
[27] Kim, D., Lee, J. K., Kang, S. O., & Ko, J. (2007). *Tetrahedron*, *63*, 1913.
[28] Choi, H., Lee, J. K., Song, K., Kang, S. O., & Ko, J. (2007). *Tetrahedron*, *63*, 3121.
[29] Kitamura, T. et al. (2004). *Chem. Mater.*, *16*, 1812.
[30] Hagberg, D. P. et al. (2006). *Chem. Commun.*, *21*, 2245.
[31] Xu, M. et al. (2008). *J. Phys. Chem. C.*, *112*, 19770.
[32] Zhang, G. et al. (2009). *Chem. Commun.*, *16*, 2200.
[33] Zeng, W. et al. (2010). *Chem. Mater.*, *22*, 1915.
[34] Xu, M. et al. (2012) *Chem. Sci.*, *3*, 976.
[35] Mao, J. et al. (2012). *Angew. Chem. Int. Ed.*, *51*, 9873.
[36] Yang, J. et al. (2012). *J. Mater. Chem.*, *222*, 4356.
[37] Cai, S. et al. (2013). *J. Mater. Chem. A*, *1*, 4772.
[38] Ning, Z. et al. (2009). *J. Phys. Chem. C*, *113*, 10313.
[39] Hao, Y. et al. (2009). *Chem. Commun.*, *27*, 4031.
[40] Koumura, N. et al. (2006). *J. Am. Chem. Soc.*, *128*, 14256.
[41] Pramjit, S., Eiamprasert, U., Surawatanawong, P., Lertturongchai, P., & Kiatisevi, S. (2015). *J. Photochem. Photobiol. A*, *260*, 1.
[42] Wan, Z. et al. (2012). *Dyes Pigments*, *95*, 41.
[43] Tian, H. et al. (2009). *Chem. Commun.*, *41*, 6288.
[44] Tian, H. et al. (2007). *Chem. Commun.*, *36*, 3743.
[45] Tian, H., Yang, X., Chen, R., Hagfeldt, A., & Sun, L. (2009) *Energy Environ. Sci.*, *2*, 674.
[46] Wu, W. et al. (2010). *J. Mater. Chem.*, *20*, 1772.
[47] Karlsson, K. M. et al. (2011). *Chem. Eur. J.*, *17*, 6415.
[48] Chen, C. et al. (2012). *J. Mater. Chem.*, *22*, 8994.
[49] Wan, Z., Jia, C., Zhou, L., Huo, W., Yao, X., & Shi, Y. (2014). *Dyes Pigments*, *109*, 96.